

Study of the consequence of excess indium in the active channel of InGaAs/InAlAs high electron mobility transistors on device properties

G. I. Ng, D. Pavlidis, M. Quiliec,^{a)} Y. J. Chan, M. D. Jaffe, and J. Singh

Center for High Frequency Microelectronics, Solid State Electronics Laboratories, Department of Electrical Engineering and Computer Science, The University of Michigan, Ann Arbor, Michigan 48109-2122

(Received 14 September 1987; accepted for publication 18 December 1987)

A study of the properties of $\text{In}_{0.52}\text{Al}_{0.48}\text{As}/\text{In}_{0.53+x}\text{Ga}_{0.47-x}\text{As}$ high electron mobility transistors is carried out for 0%, 7%, and 12% excess In values in the channel. Theoretical analysis shows that the enhanced In causes a biaxial compressive strain of 0.49% to 0.84% in the channel, increases the band-edge discontinuity from 0.437 to 0.500 eV, and reduces the carrier mass by 6%. Experimental characterizations support the theoretical predictions by demonstrating an increase of mobility from 9900 to 11 200 cm^2/Vs at 300 K, and a transconductance enhancement from 160 to at least 230 mS/mm .

Pseudomorphic high electron mobility transistors (HEMT's) have demonstrated excellent dc and rf performance.^{1,2} Devices have been made on GaAs substrates by replacing the $n\text{-AlGaAs}/\text{GaAs}$ layer with $n\text{-Al}_{0.15}\text{Ga}_{0.85}\text{As}/\text{In}_{0.15}\text{Ga}_{0.85}\text{As}$ in order to (i) profit from the higher electron mobility and velocity of InGaAs and (ii) maintain a low Al mole fraction in AlGaAs, so that persistent photoconductivity and drain current-voltage characteristics collapse at 77 K can be avoided.³ InAlAs/InGaAs HEMT's lattice matched on InP have also been reported to show extremely high transconductances (700 mS/mm at 77 K with a 1 μm gate).⁴ Good dc characteristics were also obtained with these devices by applying equal and opposite strains across the heterojunction so that lattice mismatch problems could be avoided.⁵

In order to fully understand the performance potential of pseudomorphic HEMT's, it is important to carry out a systematic study of the effect of increased In in the active channel on the mobility, sheet charge, and device transconductance. An accurate charge control model also must be developed to understand the effect of increased In on carrier properties. Details of the theoretical simulations have already been presented by the authors elsewhere.^{6,7} In this letter, we report theoretical and experimental results for such a study done on $\text{In}_{0.52}\text{Al}_{0.48}\text{As}/\text{In}_{0.53+x}\text{Ga}_{0.47-x}\text{As}$ HEMT's grown on InP substrates. This approach is expected to improve device performance over the lattice-matched case since the two-dimensional electron GaAs (2DEG) is now formed in a high InAs mole fraction layer with higher electron mobility and peak velocity. As shown in this work the conduction-band discontinuity is also increasing by at least 14% from the theoretically calculated 0.437 eV lattice-matched value when the In composition is changed from 53% to 65%. The resulting better electron confinement should therefore improve the device output resistance due to smaller carrier injection into the InAlAs buffer.

The investigated device structure is shown as an inset in Fig. 1. The layers grown on the semi-insulating InP substrate are as follows: (1) an undoped $\text{In}_{0.52}\text{Al}_{0.48}\text{As}$ buffer, (2) a lattice-matched undoped $\text{In}_{0.53}\text{Ga}_{0.47}\text{As}$, (3) a

strained undoped $\text{In}_{0.53+x}\text{Ga}_{0.47-x}\text{As}$ for the formation of the 2DEG channel, (4) an $\text{In}_{0.52}\text{Al}_{0.48}\text{As}$ spacer, (5) an n -doped $\text{In}_{0.52}\text{Al}_{0.48}\text{As}$ carrier donor layer, (6) an undoped $\text{In}_{0.52}\text{Al}_{0.48}\text{As}$ for the reduction of gate leakage, and (7) an n^+ ($2 \times 10^{18} \text{ cm}^{-3}$)- $\text{In}_{0.53}\text{Ga}_{0.47}\text{As}$ for improved source-drain ohmic contacts.

In order to control accurately the composition and thickness of each layer, the actual growth rates of the binaries involved (InAs, GaAs, AlAs) should be known. They are calibrated as a function of element III fluxes (In, Ga, Al). The relation between fluxes and measured beam equivalent pressure (BEP) is deduced from InGaAs and AlInAs lattice parameters and thickness from previous determination. The actual thickness and composition of ternaries in the samples are then deduced from BEP measurements performed just prior to growth, with an accuracy of less than 10% and 1%, respectively. Following the calibration of growth conditions, layers were grown successively with In compositions equal to 53%, 60%, and 65%. The growth rates of InGaAs and InAlAs were 1.5 and 0.98 $\mu\text{m}/\text{h}$ respec-

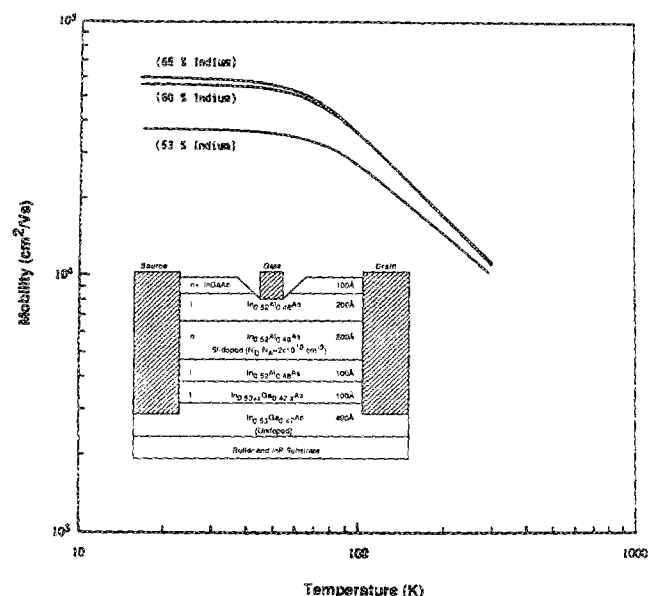


FIG. 1. Mobility-temperature characteristics for lattice-matched (53% In) and strained HEMT's. The inset shows the HEMT structure studied.

^{a)} Centre National d'Etudes des Telecommunications (CNET) 92200 Bagneux, France.

TABLE I. Effective mass (m^*/m_0), energy gap (E_g) and conduction band discontinuity (ΔE_c) as a function of In composition.

Channel material	m^*/m_0	E_g	ΔE_c
In _{0.53} Ga _{0.47} As	0.0457	0.8759	0.437
In _{0.60} Ga _{0.40} As	0.0441	0.8205	0.473
In _{0.65} Ga _{0.35} As	0.0429	0.7785	0.500

m_0 is the free-electron mass, E_g 's and ΔE_c 's are in eV.

tively and the gallium cell temperature was rapidly modified without growth interruption when passing from lattice matched to strained conditions. The estimated strain for these devices is 0%, 0.49%, and 0.84%, respectively. The thickness and doping of all layers were kept the same as shown in Fig. 1. Note that in all cases the strained channel thickness (100 Å) is considerably below the critical thickness (~200 Å) for dislocation formation. This is confirmed by the observation that in spite of the lattice mismatch in the heterostructure, the layer morphology was excellent. Hall mobility measurements in the temperature range of 300–16 K confirmed the enhanced mobility of the strained systems. Figure 1 shows that the measured mobility in this range varies between 9900 and 36 500 cm²/V s for lattice matched and 11 200 to 59 500 cm²/V s for 65% In-strained layers. The mobility enhancement is therefore of the order of 13% at room temperature and 63% at 16 K. The results suggest also that the largest improvement occurs up to 60% In; the mobility enhancement starts to tail off above this composition. The measured sheet carrier concentration of lattice matched and strained samples ranges at 16 K (53%) from 1.19×10^{12} cm⁻² to 1.29×10^{12} cm⁻² (60%) and 1.26×10^{12} cm⁻² (65%); considering the measurement errors and thickness tolerances the sheet concentration *does not therefore* depend appreciably on strain or temperature.

In order to theoretically understand the effect of channel strain on device performance, we have developed a formalism to predict the effect of strain on electron mass in the channel.⁶ This is done by using an optimized tight binding program which is capable of accurately modeling the carrier masses and energy gaps at high symmetry points of the Brillouin zone. The effect of the biaxial strain in the channel is studied by scaling the tight binding matrix elements as a function of strain using an inverse square law of the form proposed by Harrison.⁸ A scaling factor was also used to fit the known hydrostatic and shear deformation potentials.

This allowed us to determine the electron effective mass and the strained band gap. A 65:35 rule was used to obtain the band discontinuity. Next a charge control model was used which solved the Schrödinger equation and Poisson equation self-consistently taking into account the effect of strain on material parameters as discussed above.

Tables I and II summarize the results obtained by the theory. In Table I, the calculated effective mass (m^*/m_0), energy gap (E_g), and conduction-band discontinuity (ΔE_c) are shown for different In composition in the channel. The m^*/m_0 reduction and ΔE_c increase by varying the In from 53% to 65% is 6% and 14%, respectively. Table II, which shows the results of the charge control modeling of the HEMT, predicts that the total sheet density increases by about 5% at $V_g = 0.0$ V. It is interesting to note that although the carrier occupation of the first subband is higher in the presence of strain, the opposite is true for the higher subbands resulting therefore in a marginal increase of the total n_s . The higher occupation of the lowest subband level as strain is increased is expected to result in increased mobility.⁹ These expectations are consistent with our experimental observations.

Devices were processed successfully on the lattice matched and 60% In concentration wafers. The study of the 65% In sample was limited to Hall measurements only due to material and technology limitations. Mesa isolation was made using an H₃PO₄:H₂O₂:H₂O (1:1:8) solution. Ge/Au/Ni/Ti/Au ohmic contacts were deposited and followed by a two-step rapid thermal annealing at 300 and 425 °C. The contact resistivity, as determined by the transmission line method, was of the order of 2.7×10^{-6} Ω cm². Figure 2 shows the transconductance and drain-source current versus the gate-voltage V_{gs} under saturated operation ($V_{ds} = 2.5$ V) for devices with 1.2 μm (lattice matched) and 2.1 μm (strained) gate length; the gate width of the devices is 100 μm. The comparison was made with devices of different length due to the limited availability of same type transistors on the wafers. It should, however, be noted that several devices of each type were characterized and they all had the same 1 μm gate to source and gate to drain spacing. The maximum transconductance occurs for both devices at -0.2 V. At this point, the transconductance enhancement is from 160 mS/mm to at least 230 mS/mm. Since the access resistances of both devices were the same, an even more dramatic transconductance increase is expected to happen in shorter (1.2 μm) gate length devices. The current at the maximum transconductance point is for both devices of the

TABLE II. Total and subband density (n_s) variation as a function of In composition.

Channel material	$V_g = -0.4$				$V_g = 0.0$			
	total	band 0	band 1	band 2	total	band 0	band 1	band 2
In _{0.53} Ga _{0.47} As	0.555	0.331	0.112	0.061	1.116	0.742	0.202	0.092
In _{0.60} Ga _{0.40} As	0.588	0.418	0.084	0.048	1.152	0.860	0.153	0.075
In _{0.65} Ga _{0.35} As	0.614	0.486	0.062	0.037	1.179	0.944	0.121	0.061

n_s 's are in 10^{12} cm⁻², V_g 's are in volts.

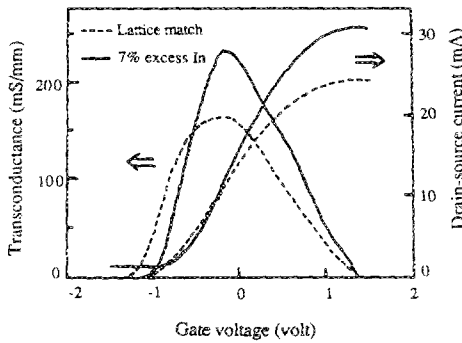


FIG. 2. Transconductance (g_m) and current-transfer (I_D) characteristics for lattice-matched (a) and strained (60% In) (b) HEMT's.

order of 110 mA/mm. The threshold voltage of the devices measured from the transfer characteristics was found to be -1.6 V.

In conclusion, our experimental results show that by introducing a strained (high In composition) channel in InGaAs/InAlAs HEMT's the mobility and transconductance can be substantially increased. These results are consistent with our theoretical expectations of increased band edge discontinuity, reduction of effective mass, and higher carrier occupation in the first subband by increasing the strain. The presented experimental and theoretical results for both lattice-matched and strained systems suggest the potential advantages of InAlAs/InGaAs strained HEMT's on InP substrates. By reducing the gate dimension of such devices and perfecting technology, it is expected that sys-

tems of this type will show excellent millimeter-wave performance.

The authors would like to acknowledge support of this work by Wright-Patterson Air Force Base contract No. F33615-87-C-1406 and U. S. Army office grant No. DAAL03-87-U-007. They would like also to thank H. F. Chau and W. P. Hong for their help in material characterization.

¹A. A. Ketterson, W. T. Masselink, J. S. Gedymin, J. Klem, C. K. Peng, W. F. Kopp, H. Morkoç, and K. R. Gleason, *IEEE Trans. Electron Devices* **ED-33**, 564 (1986).

²A. W. Swanson, *Microwaves and RF* 139 (1987).

³T. J. Drummond, R. Fischer, W. Kopp, H. Morkoç, K. Lee, and M. S. Shur, *IEEE Trans. Electron Devices* **ED-30**, 1806 (1983).

⁴K. Hirose, K. Ohata, T. Mizatani, T. Itoh, and M. Ogawa, in *Institute of Physics Conference Series No. 79* (Adam-Hilger, Bristol, U.K., 1986), Chap. 10, pp. 529-534.

⁵J. M. Kuo, B. Lalavic, and T. Y. Chang, in *Technical Digest of the International Electron Device Meeting* (IEEE, Los Angeles, CA, 1986), pp. 460-463.

⁶M. D. Jaffe, Y. Sekiguchi, J. Singh, J. J. Chan, D. Pavlidis, and M. Quillec, presented at the IEEE/Cornell Conference on "Advanced Concepts in High Speed Semiconductor Devices and Circuits," Cornell, July 1987 (to be published by IEEE, Piscataway, NJ).

⁷Y. Sekiguchi, Y. J. Chan, M. Jaffe, M. Weiss, G. I. Ng, J. Singh, M. Quillec, and D. Pavlidis, presented at the 14th Intl. Symposium on GaAs and Related Compounds, Crete, Greece, Sept. 1987 (to be published in the *Inst. of Physics Conference Series*, Adam Hilger Ltd., Bristol, U.K.).

⁸W. A. Harrison, *Electronic Structure and the Properties of Solids* (Freeman and Company, San Francisco, CA, 1980).

⁹S. Mori and T. Ando, *J. Phys. Soc. Jpn.* **48**, 865 (1980).